

---

EFDA–JET–CP(01)02-39

T.Hellsten, P.Hennequin, B.Alper, Yu.F.Baranov, A.Becoulet,  
C.Challis, E.Joffrin, N.C.Hawkes, T.C.Hender, P.J.Lomas,  
F.Orsitto, K.-D.Zastrow and JET EFDA Contributors

# Sawtoothing in Reversed Shear Plasmas



# Sawtoothing in Reversed Shear Plasmas

T.Hellsten<sup>1,2</sup>, P.Hennequin<sup>3</sup>, B.Alper<sup>4</sup>, Yu.F.Baranov<sup>4</sup>, A.Becoulet<sup>5</sup>,  
C.Challis<sup>4</sup>, E.Joffrin<sup>5</sup>, N.C.Hawkes<sup>4</sup>, T.C.Hender<sup>4</sup>, P.J.Lomas<sup>4</sup>,  
F.Orsitto<sup>1,6</sup>, K.-D.Zastrow<sup>4</sup> and JET EFDA Contributors\*

<sup>1</sup>*EFDA-Close Support Unit, Abingdon, OX14 3EA, UK*

<sup>2</sup>*KTH Association Euratom/VR, SE-10044 Stockholm, Sweden*

<sup>3</sup>*Euratom/ UKAEA Fusion Association, Culham Science Centre, Abingdon, OX14 3DB, UK*

<sup>4</sup>*LPTP, UMR7648, Ecole Polytechnique, F-91128 Palaiseau, France*

<sup>5</sup>*Association Euratom-CEA, Cadarache, F-130108, St. Paul lez Durance, France*

<sup>6</sup>*Helsinki University of Technology, Association Euratom-Tekes, Finland*

<sup>7</sup>*Association Euratom-ENEA, I-00044 Frascati, Italy*

*\*See appendix of the paper by J.Pamela "Overview of recent JET results",  
Proceedings of the IAEA conference on Fusion Energy, Sorrento 2000*

Preprint of Paper to be submitted for publication in Proceedings of the  
EPS Conference,  
(Madeira, Portugal 18-22 June 2001)

“This document is intended for publication in the open literature. It is made available on the understanding that it may not be further circulated and extracts or references may not be published prior to publication of the original when applicable, or without the consent of the Publications Officer, EFDA, Culham Science Centre, Abingdon, Oxon, OX14 3DB, UK.”

“Enquiries about Copyright and reproduction should be addressed to the Publications Officer, EFDA, Culham Science Centre, Abingdon, Oxon, OX14 3DB, UK.”

## ABSTRACT

Discharges with internal transport barriers, ITBs, having a high fraction of bootstrap current is a promising route towards quasi-steady state operation of tokamaks. The underlying hypothesis for forming and sustaining ITBs is that the turbulence governing the transport under normal plasma conditions is suppressed by reversed magnetic shear and/or  $\mathbf{E} \times \mathbf{B}$ -shear [1]. It has been found that the shape of the  $q$ -profile is important for achieving ITBs, but the role of the locations of rational (integer)  $q$ -values and the minimum  $q$  still remain unclear. Sawtooth-like modes have been seen in ITB experiments [2-4]. In recent JET ITB-experiments produced by LHCD-preheat, large ( $m = 2$ ,  $n = 1$ ) and (3,1) sawtooth-like modes appear in the reversed shear region of the barrier during the high performance phase when  $1 < q_{\min} < 2$  and  $2 < q_{\min} < 3$ , respectively. These modes depend on the heating method. Minority heating of hydrogen produces in general a low sawtooth frequency with high amplitude in  $\Delta T_e$ , whereas minority heating of  $^3\text{He}$  and direct electron heating with ICRH produce higher frequency with lower amplitude. Continuous modes produced by the sawteeth are seen to locally flatten the angular velocity and thereby increase the second derivative of flow shear, which may reduce the turbulence. Depending on the size of the island the confinement could then either improve or deteriorate.

The localisation of the MHD-modes around rational  $q$ -surfaces can be used for reconstructing the  $q$ -profiles. The change of the current distribution in the centre can be qualitatively determined from the motion of the inversion radius during sawtoothing. For mild sawteeth an expansion of the inversion radius is often seen, which implies that a reduction of the central current occurs in spite of sawtoothing and current diffusion. Continuous modes triggered by stronger sawteeth usually contract the inversion radius and thus enhance the current penetration through the barrier.

## 1. SAWTOOTHING

Large sawtooth-like modes appear in discharge Pulse No: 51053 during the main heating phase with minority hydrogen ICRH and NBI heating. The variations of some of the main parameters in the later part of the discharge are shown in Fig. 1. The plasma current is 3.1MA, the magnetic field at centre 3.4T and the RF-frequency 51MHz producing nearly on axis heating. Density, electron and ion temperature barriers develop. The electron and ion temperatures are similar. The foot of the transport barrier can be seen from ion temperature measurements with the active charge exchange spectroscopy, from electron temperature measurements with the 48 channels polychromator, and density measurements from the LIDAR, which all give barriers with the foot at about 3.35m, Fig. 2. The density at the magnetic axis is fairly constant during 8-9.8s, whereas the density gradient in the barrier increases.

A number of large sawtooth-like modes appear between  $8 < t < 9$ s with a dominant  $n = 1$  component, which increases with time, Fig. 3. The sawteeth at  $t = 9.03$ s and  $9.6$ s are followed by continuous modes with large  $n = 1$  and  $n = 2$  components for about 200ms. The MHD amplitude of  $B$  at the crashes are for these modes 20 times higher than for the large sawtooth at  $t = 8.9$ s, which

in its turn is about 3 times higher than the earlier ones. The continuous modes reduce the confinement, which can be obtained by studying the pressure gradient.

Between  $t = 7.0\text{s}$  and  $8.86\text{s}$  the inversion radius of the sawteeth expands from  $R = 3.18\text{m}$  to  $3.22\text{m}$ . During the period when the large sawteeth producing continuous modes occurs the inversion radius contracts, at  $t = 9.6\text{s}$  it has contracted to  $R = 3.18\text{m}$ . The changes in  $T_e$  before and after the sawteeth are similar even though the magnitude in MHD activity differ considerably. Unlike normal (1, 1)-sawteeth these do not produce flat temperature profiles inside the reversal surface after the crashes. The temperature profiles are still strongly peaked and only a modest reduction of the temperature gradients take place. The largest change in the electron temperature gradient occurs in a narrow region around the inversion radius, Fig. 3.

An island develops in the barrier region after the large sawteeth at  $t = 9.03\text{s}$  and  $9.6\text{s}$ , reducing the confinement. The line integrated soft x-ray emission, Fig. 5, is consistent with an island with an even poloidal mode number. EFIT calculations of the equilibrium, with magnetics only, give  $q = 2$  in the centre. The measured mode frequency agrees with the angular velocity of an  $n = 1$  mode at the position of the inner  $q = 2$  surface at  $R = 3.2\text{m}$ .

During  $8.2 < t < 8.4\text{s}$  and  $9.03 < t < 9.6\text{s}$  smaller annular oscillations of  $T_e$  not affecting the core take place with an inversion radius at  $R = 3.35\text{m}$  and  $R = 3.30\text{m}$ , respectively, corresponding to the  $q = 2$  surface in the positive shear region. These modes are also associated with dominating  $n = 1$ , but the level is low. The presence of two  $q = 2$  surfaces implies that the discharge had a reversed magnetic shear. Calculations of the  $q$ -profile using MSE measurements for similar discharges are in agreement with formation of reversed magnetic shear.

The bootstrap current in the barrier region increases with the density and temperature gradients as the confinement improves, Fig. 6. The observed expansion of the inversion radius at the inner  $q = 2$  ( $q = 3$ ) surfaces during the build up of the bootstrap current is consistent with an increase of the total current inside the inversion radius, but a reduction of the current inside the former location of the inversion radius. The reduction of the central current takes place in spite of the sawtoothing, which reduces the current gradients and current diffusion. Thus the redistribution of the current near the rational  $q$ -surface in the reversed shear region of the barrier due to sawtoothing is counteracted. This can e. g. be achieved by the build up of bootstrap currents or currents produced by LHCD in the barrier region. In Pulse No: 51053 there were no LHCD during the main heating phase.

The island produced by the large sawteeth at  $t = 9.03\text{s}$  flattens the angular velocity to  $5.2 \cdot 10^4$  rad/s in the barrier at  $3.2 < R < 3.3\text{m}$ , Fig. 2. Also the electron temperature outside the inversion radius are flattened, but is steepened up inside it, which can be deduced from the separation of the different ECE-channels in Fig. 3. The steepening of  $T_e$  inside the inversion surface is consistent with an influx of current towards the centre. The magnetics show an oscillating signal with a frequency of  $7.5\text{kHz}$  during the continuous mode. The latter frequency is close to the local angular velocity at  $R = 3.25\text{m}$  where the flattening of the angular velocity takes place, consistent with a

mode rotating with the plasma at the inversion radius.

Similar sawtooth behaviour in the main heating phase with an expanding inversion surface is seen in Pulse No: 53782 for an ICRH scenario using 37MHz in deuterium plasma with a magnetic field of 3.45T and plasma current of 2MA producing direct electron heating without fast ions. An electron ITB with  $T_e(0) = 8.5\text{keV}$  is produced with LHCD, ICRH and NBI, Fig. 7. Due to lower central NBI-power than in Pulse No: 51053 there is no strong ion-ITB. The ion temperature measured with the crystal spectrometer is 4keV. The averaged time between sawteeth crashes is about half of that in Pulse No: 51053. Before ICRH starts the sawteeth produced during NBI and LH heating are small with a short time between the crashes, of the order of 70ms. The q-profile measured with polarimetry is consistent with an inversion surface at the  $q = 3$  surface. For some of the sawteeth after  $t = 5.98\text{s}$  continuous modes are produced with large  $n = 1$  activity resulting in a contraction of the barrier. As the barrier contracts the previous flat central temperature profile peaks up, consistent with current penetration, but the gradients in the barriers are reduced. The continuous modes appear for this discharge at a low  $\beta$ -value below 0.7%.

Small frequent sawteeth are also produced in Pulse No: 53844 during  $^3\text{He}$  minority heating in deuterium plasma, with similar parameters as in Pulse No: 53782 except for a low  $^3\text{He}$  concentration. The amplitude and frequency of these sawteeth, Fig. 8, change as the  $^3\text{He}$  cyclotron resonance approaches the inversion surface from the high field side due to the increasing magnetic field. The location of the inversion radius is roughly the same, but the temperature gradient inside the inversion radius is smaller for the frequent sawteeth. The change in amplitude and frequency are consistent with that the frequency depends on the power deposition and the fast ion content near the inversion radius and the amplitude in  $\Delta T_e$  on the gradient inside the inversion radius similar to normal (1,1)-sawteeth [5, 6].

## CONCLUSIONS AND DISCUSSIONS

The temperature and density profiles remain peaked after the sawtooth crashes in reversed shear ITB plasmas, only a local flattening near the inversion radius takes place. The variation of the sawteeth like modes depends on the gradients in the barrier and heating method. In discharge #51053 the  $\beta$ -value increases slowly after 8.2s and reaches only 0.97% before the first large sawteeth, whereas the density profile peaks up continuously. Since the modes appear both at low and high  $\beta$ -values and the strength of the MHD activity increases as the density peaking increases, it seems therefore likely that the strength of the sawteeth are related to the density gradients and bootstrap current in the barrier region. In discharge #51053 the mode structure from the soft x-ray is consistent with a single island near the inner  $q=2$  surface, the strong gradients in the barrier between the two  $q=2$  surfaces, the localised changes of the  $T_e$ -profile around the inner  $q=2$  surface and a mode rotating with the plasma at the local velocity indicate that the effect of the mode dominates at the inner  $q=2$  surface. Correlation analyses reveal often that the MHD activities at the two  $q=2$  ( $q=3$ ) surfaces are correlated [7]. The mode coupling may still be important for the dynamics of the

modes although the modes do not cause full reconnection between the two resonant surfaces like normal double tearing modes.

The expansion of the inversion radius at the  $q=2$  surface in the reversed shear region is consistent with that the current in the centre is reduced during mild sawteeth, which could be caused by increasing bootstrap driven current in the barrier. The continuous modes appearing after strong sawteeth crashes results often in an increasing current in the centre. These effects produce a self-organising mechanism for the current profile, which can facilitate quasi-steady state operation. However, if the barrier steepens up too much the heating and/or fuelling have to be reduced in order to avoid violent instabilities, which can lead to disruption.

## REFERENCES

- [1]. K.H.Burrell, Phys. Plasmas **4** (1997)1499.
- [2]. M. de Baar et al, Phys. Rev. Lett. **78** (1997) 4573.
- [3]. R.F.G.Meulenbroeks et al, Physics of Plasmas **6** (1999) 3898.
- [4]. S.Günter et al, Nucl. Fusion **40** (2000) 1541.
- [5]. D.Campbell et al, Phys. Rev. Lett. **60**, 2148 (1988).
- [6]. P.Helander et al, Phys. Plasmas **6** (1997) 2181.
- [7]. P.Hennequin et al, this conf. (28th EPS).



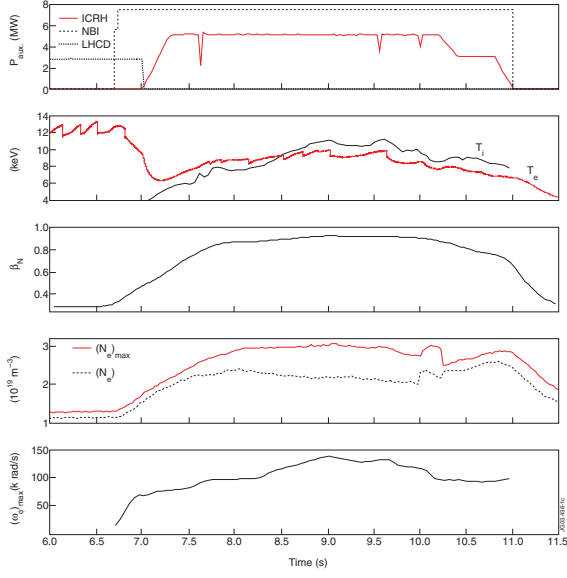


Figure 1: Time traces of Pulse No: 51053 ( $\omega_p$  in  $10^4$  rad/s).

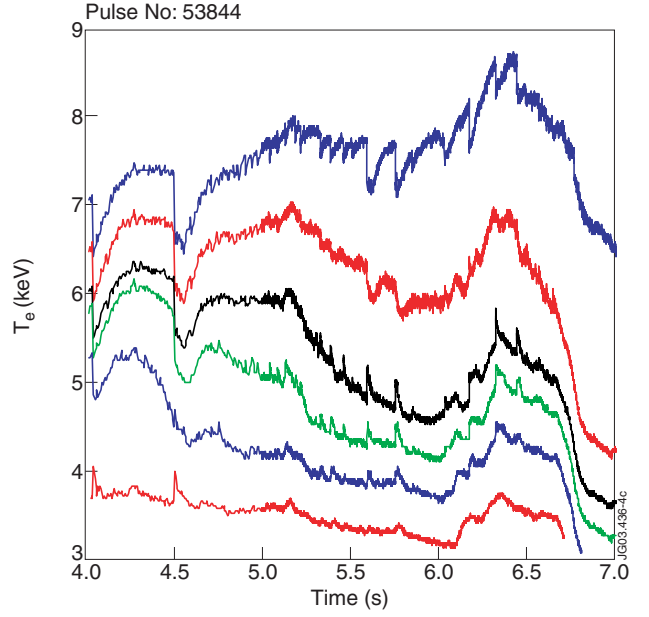


Figure 2:  $\omega_p$ ,  $T_e$ ,  $T_i$  and  $n_e$  in Pulse No: 51053 before (solid) and after (dashed) the sawtooth crash at  $t = 4.9$ s.

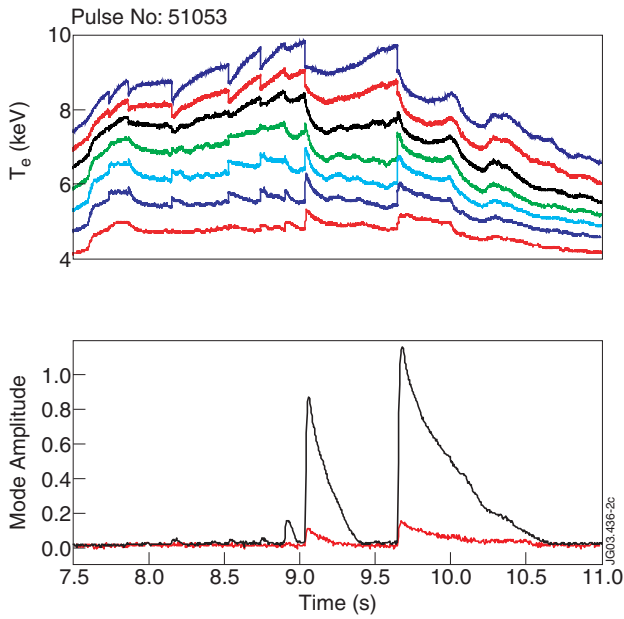


Figure 3:  $T_e$  and amplitudes of the  $n = 1$  (solid) and  $n = 2$  (dashed) modes in Pulse No: 51053.

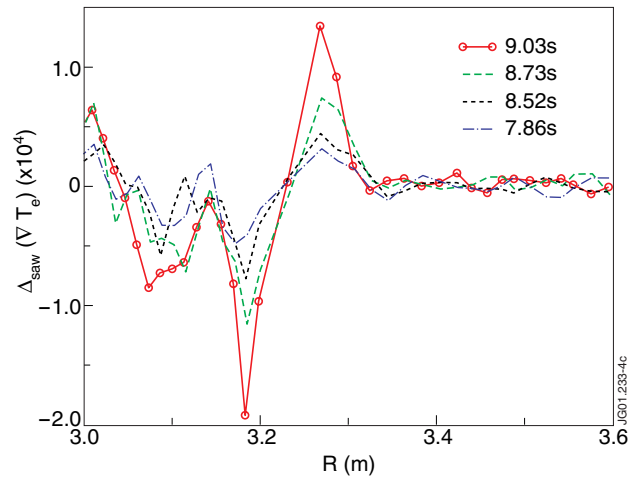


Figure 4: The radial change in the change in  $T_e$  before and after a sawtooth  $\Delta T_e(r_{n+1}) - \Delta T_e(r_n)$ .

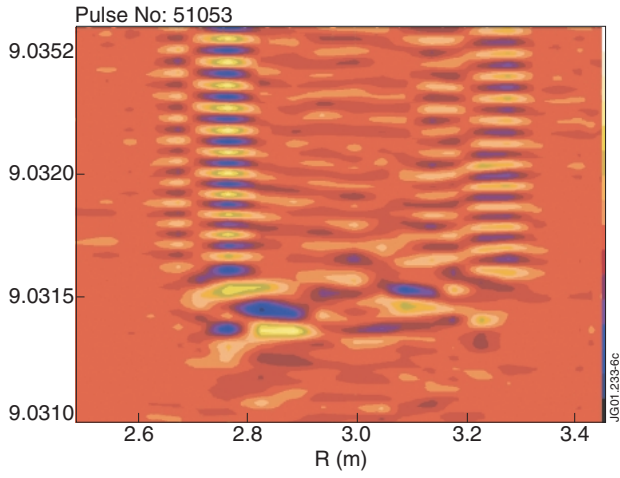


Figure 5: Line integrated SXR emission versus time (y-axis) after filtering out equilibrium emission profile during the continuous mode after the sawtooth crash at  $t = 9.04$ .

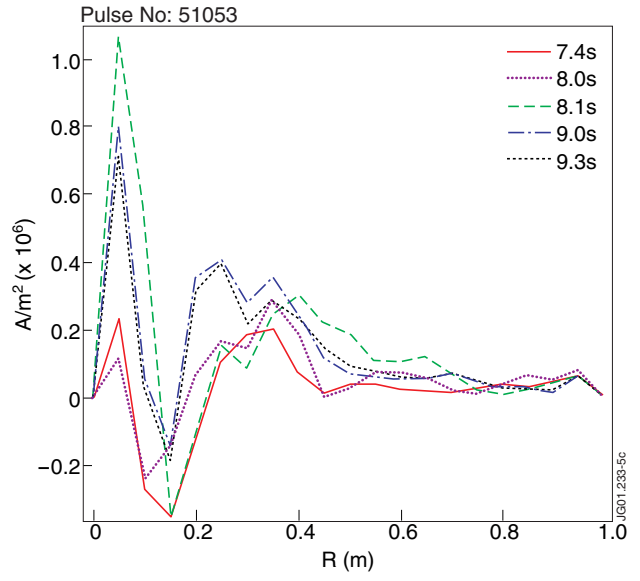


Figure 6: Bootstrap current as calculated with CHAIN 2.

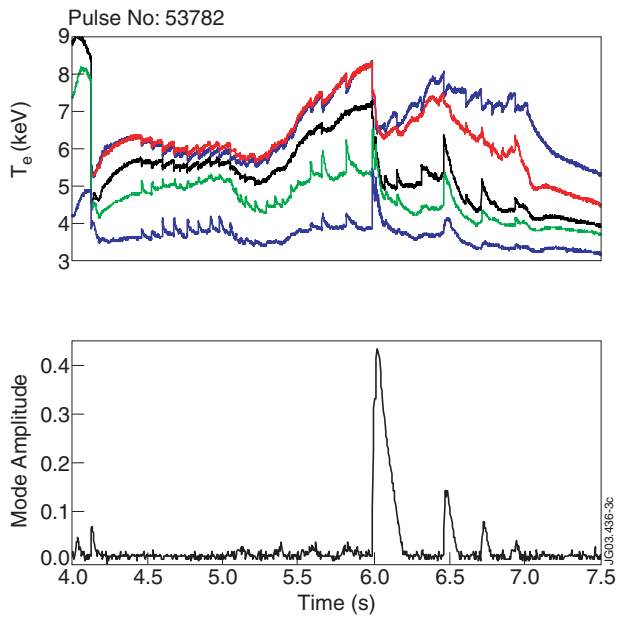


Figure 7:  $T_e$  and amplitude of the  $n = 1$  mode in Pulse No: 53782.

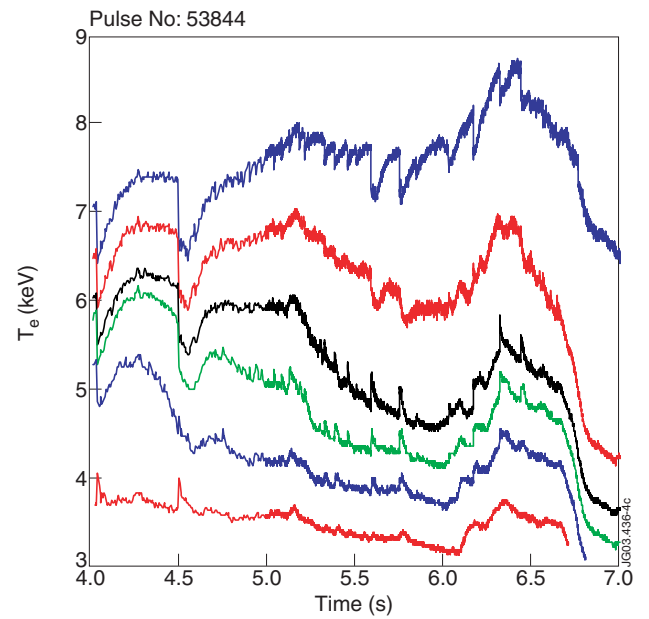


Figure 8:  $T_e$  for Pulse No: 53844.